AUSTRAL-MAGALLANES BASIN EVOLUTION: A MODEL BASED ON U-PB DETRITAL ZIRCON GEOCHRONOLOGY AND STRUCTURAL DATA

Juan F. Albano[1], Laura Lombardi[1], Emilio Rocha[2,3], Jonathan Tobal[1], Julie C. Fosdick[4], Andrea L. Stevens Goddard[5], Rebecca A. VanderLeest[6], Miguel Ramos[1], Pablo Giampaoli[2] , Pedro Kress[2], Fernanda Raggio[2] and Matías C. Ghiglione[1]

1: Universidad de Buenos Aires. juanf.albano@gmail.com, lauralombardi@live.com.ar, jonathantobal@gmail.com, licmiguelramos@gmail.com, mcghiglione@gmail.com

2: YPF S.A. pablo.giampaoli@ypf.com, pkress@ypf.com, maria.raggio@ypf.com

3: Currently at Pluspetrol S.A. emilio.rocha@pluspetrol.com

4: University of Connecticut. julie.fosdick@uconn.edu

5: Indiana University. alsg@iu.edu

6: West Texas A&M University. rvanderleest@wtamu.edu

Keywords: Austral-Magallanes Basin, kinematic evolution, structural modelling, U-Pb zircon geochronology, Southern Patagonian Andes fold-thrust belt, burial history

RESUMEN

El inicio de la fase de antepaís de cuenca Austral-Magallanes se reconoce por la aparición de turbiditas arenosas ubicuas sobre los depósitos precedentes de grano fino de la fase de SAG. En el área estudiada, el registro estratigráfico de la fase de antepaís comprende un apilamiento de depósitos marinos poco que superan los 5000 m de espesor. Utilizando geocronología U-Pb en circones detrítico sobre diez muestras de arenisca distribuidas en todo el espesor de los depósitos de antepaís de los Andes Patagónicos Australes a 51°20'S de latitud, calculamos las edades máximas de depositación (MDA). La muestra más antigua, con una edad de 96,0 ± 1,5 Ma, corresponde a los primeros bancos de areniscas de la Formación Punta Barrosa, mientras que la más reciente, con una edad de 41 ± 3 Ma proviene de la Formación Río Turbio superior. Estos nuevos datos contribuyen a completar la información geocronológica existente para la región de Última Esperanza. Vinculando los datos de procedencia de circones detríticos nuevos y de publicaciones previas, el análisis de MDAs, los datos de termocronología y los datos estratigráficos con una sección estructural balanceada, proponemos un modelo paso a paso que combina la evolución cinemática del frente orogénico de la faja plegada y corrida con la historia de la cuenca. Se reconoce un escenario de frente orogénico para el Cretácico Superior, así como dos eventos menores de levantamiento para el Eoceno, seguidos por un evento de exhumación tectónica mayor durante Mioceno. También modelamos una historia de soterramiento que nos permitió identificar que la principal roca madre de la cuenca alcanzó la ventana de generación de petróleo y gas entre el Campaniano y el Maastrichtiano y su mayor grado de madurez fue en el Paleógeno-principios del Eoceno.

INTRODUCTION

The Patagonian fold-thrust belt exposes thick Late Cretaceous foreland sequences from the Austral-Magallanes basin (Fig. 1). A ~5000 m thick stratigraphic column is recognized in the study area at ~51°S, recording an overall regressive trend from basal distal turbiditic deposits related to a basin floor setting to shallow marine and deltaic / fluvial-deltaic deposits (Cecioni 1957; Katz 1963; Malumián *et al.* 2000; Arbe 2002; Fildani y Hessler 2005; Romans *et al.* 2011; Schwartz and Graham 2015). In order to understand the depositional mechanisms and its evolution, these deposits have been described and analyzed by several authors, taking into account different aspects, such as energy and orientation of paleoflows, sediment routing, sedimentation rates, among other variables (e.g., Sohn *et al.* 2002; Crane and Lowe 2008; Hubbard *et al.* 2008, 2010; Armitage *et al.* 2009; Jobe *et al.* 2010; Bernhardt *et al.* 2011; Schwartz *et al.* 2016). However, structural analysis, restoration methodologies, interplay between tectonic growth and sedimentation, structural inversion, etc. are less frequent in the literature (e.g., Fildani *et al.* 2003; Ghiglione *et al.* 2009, 2014; Fosdick *et al.* 2011; Giacosa *et al.* 2012; Likerman *et al.* 2013; Sachse *et al.* 2016a).

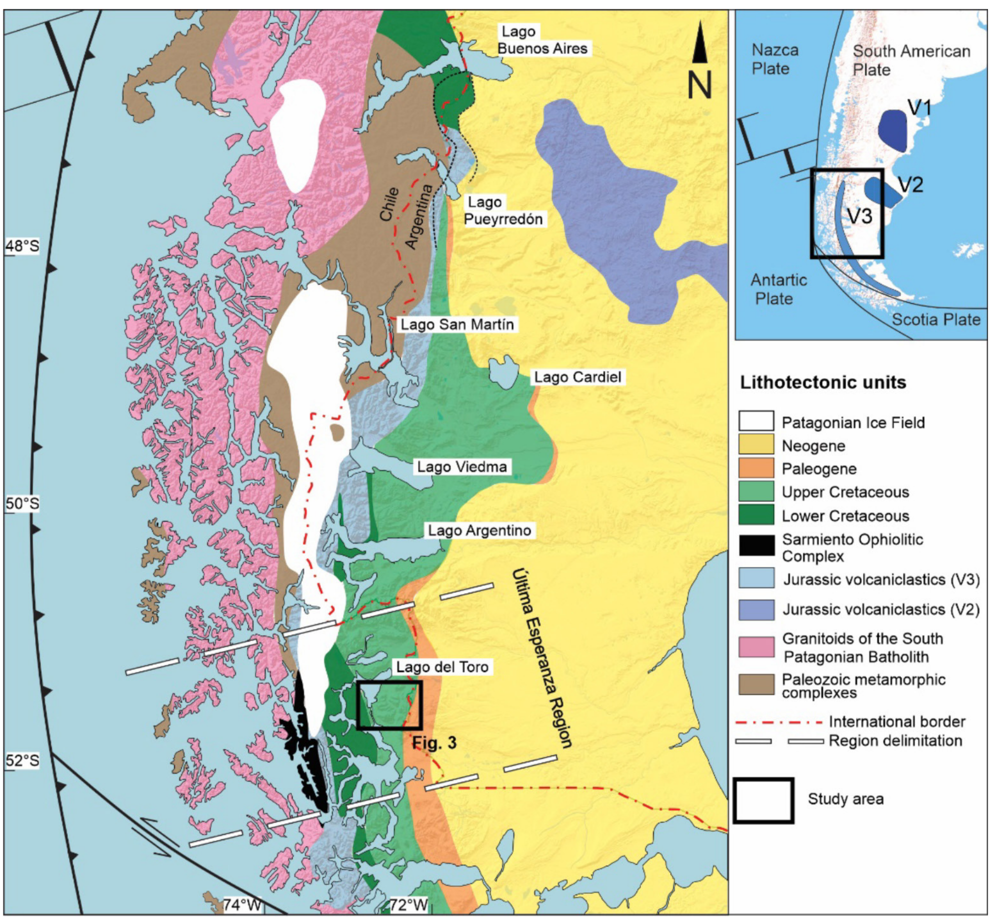

Figure 1. Regional geologic map of the southern Patagonian Andes. Lithotectonic units are simplified from SERNAGEOMIN (2003) and SEGEMAR (2003). Jurassic extensional volcanism episodes (V1, V2 and V3) are from Pankhurst *et al.* (2000).

Early stratigraphic studies have used biostratigraphic data to estimate depositional ages (Hünicken 1955; Winn and Dott 1979; Riccardi and Rolleri 1980; Russo *et al.* 1980; Malumián and Caramés 1997; Aguirre-Urreta 2002; Malumián and Náñez 2011). Over the last 20 years, U-Pb zircon dating has provided more accurate results (Fildani *et al.* 2003; Romans *et al.* 2010, Fosdick *et al.* 2011, 2015a, 2020; Bernhardt *et al.* 2012; Schwartz *et al.* 2016; Malkowski *et al.* 2015, 2016, 2018; Daniels *et al.* 2018, 2019; Sickmann *et al.* 2018; Leonard *et al.* 2020).

Late Cretaceous to early Paleocene uninterrupted sedimentation contrasts with the presence of unconformities and hiatuses observed from Paleocene time onwards. The Cenozoic record presents at least two unconformities, related to a basin-wide Upper Paleocene- Lower Eocene hiatus and another one, less regional, spanning Late Oligocene-early Miocene time. The thickness of the section eroded during Paleogene times and the corresponding temporal hiatus are still unknown and, although some thermochronological and chronostratigraphic studies have been carried out during the last decade, the results obtained are very variable with estimates of eroded thickness spreading from ~750 m up to 5000 m (Fosdick *et al.* 2015b; Ali 2016; George *et al.* 2020). The Late Oligocene-early Miocene unconformity is less marked, both in terms of eroded section and hiatus, it marks the beginning of the major stage of crustal shortening in the study area in agreement with exhumation data (Fosdick *et al.* 2013, Leonard *et al.* 2020; this study).

In this paper, we present a multidisciplinary study combining new U-Pb ages on detrital zircons together with the existing chronostratigraphic framework of the area. In addition, we present a balanced kinematic-structural model of the eastern margin of the fold-thrust belt at ~50°20’ S latitude showing the convergence and overlap of different structural mechanisms. Detrital zircons data is used to adjust the stratigraphic framework, providing new MDAs from Punta Barrosa Formation (onset of foreland stage) up to Río Turbio Formation. In short, the presence of unconformities and thermochronological information from previous studies helped us to bracket the timing of shortening phases for the kinematic model, allowing a balanced step by step palinspastic reconstruction. Basin information compiled in this work also allowed us to obtain a burial history and maturity model of source rocks.

STRATIGRAPHY OF THE STUDIED LOCALITIES

Three stratigraphic sections have been measured and described for this study aimed at constructing a composite and continuous Upper Jurassic–early Miocene stratigraphic section (Figs. 2 and 3): i, Cerro Castillo and La Península; ii, Arroyo Picana; and iii, Río Turbio.

The basement encompasses low-grade metamorphic rocks from a turbiditic protolith, ranging in age from Devonian to Triassic and grouped into the “Eastern Andean Metamorphic Complex” (EAMC) (Dalziel 1981; Mpodozis and Ramos 1990; Hervé *et al.* 2003; Calderón *et al.* 2016; Suárez *et al.* 2019). These rocks do not appear in the study area, the nearest outcrops are located ~70 km to the west (Fig. 1). The oldest emerged unit of the study area is the Tobífera Formation. It generally crops out in western area of the orogen; however, a small outcrop of this unit is identified in the core of the Rio Rincón Anticline (Fig. 3). The unit is included in the the Chon Aike LIP with equivalents throughout Patagonia and represents the Late Jurassic deposits of the synrift stage of the basin (Pankhurst *et al.* 1995, 2000; Calderón *et al.* 2007). It is built up predominantly of rhyolitic ignimbrites, rhyolitic or andesitic tuffs and lava, interbedded with sediment gravity-flow deposits, dark shale and rare pillow basalt layers (Thomas 1949; Wilson 1991).

Lower Cretaceous sedimentary marine units correspond to the Zapata Formation which overlays the Tobífera rhyolitic flows, elsewhere equivalent to Río Mayer, Erezcano and the Lower Palemo Aike Formation. It is represented by black, finely laminated and massive mudstone interbedded with thin siltstones and very fine-grained sandstones from a marine environment (Katz 1963; Wilson 1991; Aguirre-Urreta 2002; Calderón *et al.* 2007). Due to its high content of organic matter in its lower section, this unit represents the main oil-source rock of the basin.

The contact between Zapata and Punta Barrosa Formations is characterized by the appearance of turbiditic sandstones beds in the basin with medium grain composition with a thickness between 30 and 120 cm (Cecioni 1957; Katz 1963; Wilson 1991, Fildani *et al.* 2003; Fildani and Hessler 2005; Fosdick *et al.* 2011; Romans *et al.* 2011; Malkowski *et al.* 2015). We recognized the boundary between Zapata and Punta Barrosa Formations in a previously undescribed profile along La Península location, were the transition from sag to foreland units occur in a ~30 m stratigraphic interval. Overlaying Punta Barrosa Formation bears a thickness of ~350 m, composed of sandstone beds up to 1 m thick and hundreds of meters of lateral extension interpreted as from unconfined turbiditic flows interfingering with hemipelagic mudstones with few centimeters thick. Each sandstone bed shows basal erosion followed by normal gradation (from medium-to coarse-grained at the base to fine-grained and very fine-grained towards the top).

Punta Barrosa is conformably overlain by the Cerro Toro Formation with turbiditic sandstones in the lower and middle section interbedded with shales. It contains a higher percentage of mudstone than the Punta Barrosa Formation. Within the upper section of the Cerro Toro Formation, channelized conglomeratic deposits are recorded known as the Lago Sofía member (Katz 1963). In the study area, we recognized almost 400 m (of a total ~1300 m formational thickness) of this stratified clast-supported with sandy matrix conglomerate.

The boundary between Cerro Toro and Tres Pasos Formation is transitional. Tres Pasos is mainly built up by turbiditic sequences interbedded with shales. This unite was deposited in a slope environment and not in the abyssal plain like the underlying Cerro Toro Formation (Katz 1963; Shultz *et al.* 2005; Hubbard *et al.* 2010; Romans *et al.* 2011). The lower section is characterized by the presence of amalgamated turbiditic channel deposits that conforms up to 25 m thick and 200 to 400 m of lateral extension bodies of coarse to pebbly sandstones. In the upper section, these coarse deposits become less abundant and fine to medium sandstones with

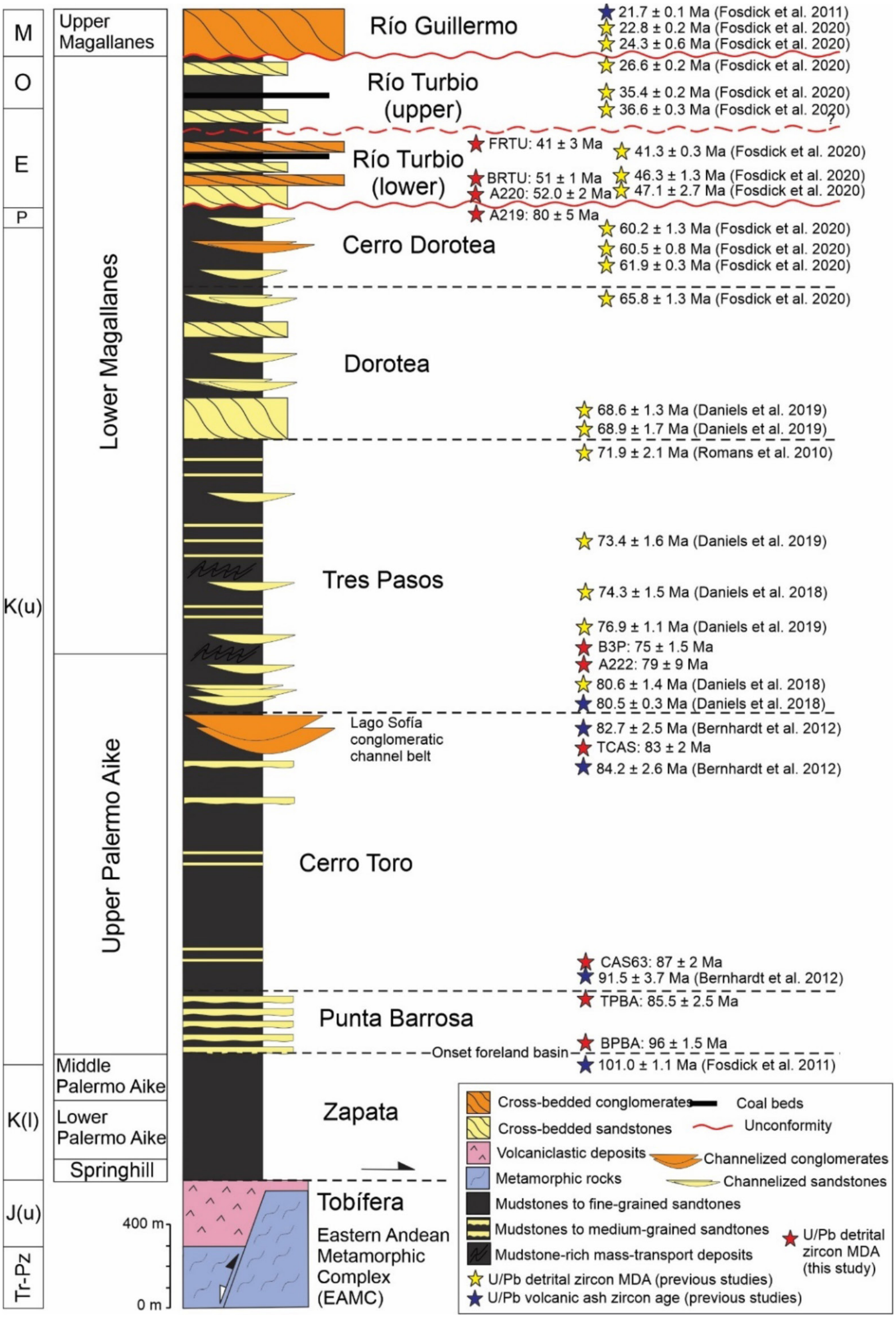

Figure 2. Compiled stratigraphic column for the studied locations. Lithologies and stratigraphic thicknesses are taken from Wilson (1991), Fildani and Hessler (2005), Hubbard *et al.* (2008, 2010), Romans *et al.* (2010), Fosdick *et al.* (2011), Malumián *et al.* (2000), Schwartz and Graham (2015) and own fieldwork. Traditional subsurface unit names are included in the left column. Acronyms on the timescale to the left are: Tr-Pz Paleozoic and Triassic, J(u) Upper Jurassic, K(l) Lower Cretaceous, K(u) Upper Cretaceous, P Paleocene, E Eocene, O Oligocene, M Miocene.

mudstones interbedded deposits predominate, interpreted as unconfined turbidites. Campanian Tres Pasos Formation, equivalent to Cerro Cazador Formation, could be correlated to the north with Alta Vista and Anita Formations, outcropping on the southern margin of Lago Argentino (Leanza 1972; Macellari *et al.* 1989; Arbe 2002). The Tres Pasos Formation is well exposed along a >100 km north–south oriented, eastward-dipping outcrop belt in the Ultima Esperanza region known as the frontal monocline (Fig. 3).

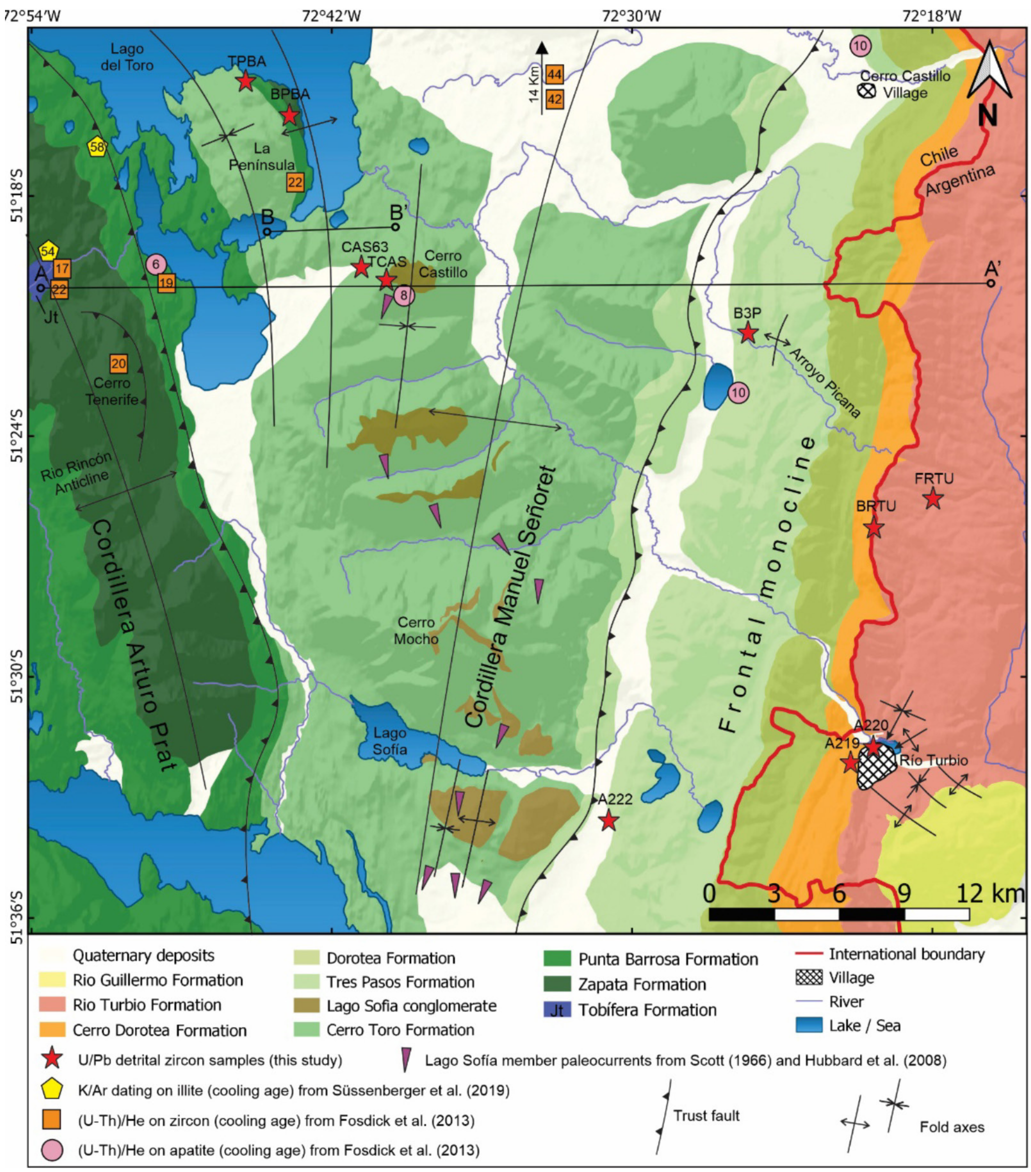

Figure 3. Geological map of the study area in the Ultima Esperanza region (see Fig. 1 for location) based on collected field data, and on Wilson (1991), Malumián *et al.* (2000), Fildani and Hessler (2005), Hubbard *et al.* (2010), Fosdick *et al.* (2011), Romans *et al.* (2011), Bernhardt *et al.* (2012) and Daniels *et al.* (2018).

Dorotea are the topsets of the Tres Pasos Formation, it is composed mainly of sandy and conglomeratic channel deposits with minor mudstone interbedded. It contains abundant plant fossils (leaves and trunks) as well as bivalves, brachiopods, gastropods and the remains of vertebrates. The fossiliferous associations correspond to shallow marine facies or marine-continental intercalations (Malumián *et al.* 2000) and the depositional environment is interpreted as a shelf-edge delta that provides sediment to the slope and basin plain (Covault *et al.* 2009; Hubbard *et al.* 2010; Romans *et al.* 2011; Schwartz and Graham 2015). Dorotea Formation is overlain in concordant contact by the laterally discontinuous Cerro Dorotea Formation, both units constitute a continuous regressive sequence of ~1100 m thick outcropping in the frontal monocline with a ~ 20 ° east-dipping angle.

The Rio Turbio Formation can be divided into two members, where the lower one is characterized by an overall coarser lithology with conglomerates and coarse sandstones and the upper one is dominated by sandstones and mudstones. The lower section corresponds to a subaqueous fluvial to fan delta environment whereas the upper one represents a coastal plain environment. Both members contain several marine and continental fossils and up to five levels of coal beds associated with different episodes of marine transgressions (Feruglio 1938; Hünicken 1955; Leanza 1972; Russo *et al.* 1980; Malumián *et al.* 1997, 2000). Its outcrops appear in the southwestern margin of Santa Cruz Province of Argentina, presenting an eastward-dipping belt that gradually decrease in dip to the foreland.

The youngest unit of the analyzed profile is the upper Oligocene - lower Miocene Río Guillermo Formation (Leanza 1972; Riccardi and Rolleri 1980; Leonard *et al.* 2020). Composed mainly of fluvial conglomerates, it overlays unconformably Río Turbio Formation. Unlike the underlying formation, this one is deposited in a fully continental environment (Malumián *et al.* 2000).

In summary, deep marine Cretaceous deposits represent the main fill of the basin (~5000 m in the studied area), mainly composed of large turbiditic sequences that in some levels register abrupt increases in flow intensity as is the case of the sandy Punta Barrosa Formation and Lago Sofia conglomerate channels. From Campanian time onwards, a sustained regression process begins going from an abyssal plain (Cerro Toro Formation) to a slope environment (Tres Pasos Formation), followed by deltaic deposits (Dorotea and Cerro Dorotea Formations), coastal deposits for Palocene and Eocene time (Río Turbio Formation) and finally, continental Miocene deposits (Río Guillermo Formation). At least two sedimentation hiatuses are recorded in the column, the most important one of ~15 Myr in Paleocene time and a minor one of ~2 Myr towards the end of Oligocene, beginning of Miocene time (Fosdick *et al.* 2011, 2020; Leonard *et al.* 2020). There could be a possible third hiatus between both members of the Río Turbio Formation or several hiatuses within this formation, evidenced by changes in fossiliferous associations and temporal jumps in detrital zircons U-Pb depositional ages (Malumián *et al.* 2000; Fosdick *et al.* 2015a, 2020).

DETRITAL ZIRCON GEOCHRONOLOGY

Methods

The zircon separates were obtained by the LaTeAndes laboratory (Salta, Argentina) using 4 to 5 kgs medium to coarse sandstones samples taken in the field. The process of zircon extraction involves crushing, density, and magnetic separation techniques in order to obtain the non-magnetic heavy minerals and finally take the zircons by hand picking. The U-Pb analysis was conducted at the London Geochronology Centre with an LA-ICP-MS (Laser Ablation - Inductively Coupled Plasma Mass Spectrometry). This technique allows to perform punctual isotopic analyses over individual zircon grains.

The detrital nature of the rocks prevents from calculating an absolute depositional age, instead, using the youngest zircons found on each sample (Fig. 4) we can estimate the MDA with two different methods which are: (i) the weighted average algorithm of the youngest cluster of overlapping 1σ or 2σ uncertainties and (ii) the youngest single zircon age. MDA algorithms were calculated using Isoplot (Ludwig 2003). In some cases, for method (i), the youngest single zircon was not taken into account in order to obtain a larger cluster for a better statistical value (e.g., samples TCAS, B3P and A222). Weighted average algorithm yields more statistically reliable MDAs than using only one zircon (Dickinson and Gehrels 2009) but, in some cases the youngest individual ages of the sample did not overlap with each other and the younger single zircon age results more coherent with previous paleontological and geochronological work than the youngest overlapping cluster (e.g., samples A219 and BRTU).

Maximum depositional ages of the sequence

The oldest analyzed unit with U-Pb geochronology in this study is the Punta Barrosa Formation, for which we obtained an MDA of 96.0 ± 1.5 Ma by calculating the weighted average of the 6 youngest zircons of the BPBA sample (Fig. 4), taken from the first sandstone beds of the unite. The resulting age is younger than that obtained previously (101 ± 1 Ma) by Fosdick *et al.* (2011) from tuff zircons, and older than that obtained (92 ± 1 Ma) by Fildani *et al.* (2003) from detrital zircons. The boundary between Zapata and Punta Barrosa was originally described as abrupt (Cecioni 1957; Katz, 1963; Wilson 1991), however, later studies estimate a transition during which 150 m of sediments were deposited, without a precise boundary (Fildani and Hessler 2005). We agree with this latter proposal as observed in the outcrops of La Peninsula, although we interpret a thinner (20 to 30 m) transitional interval, characterized by an increase of sandstone beds both in thickness and grain size within deep marine mudstone background sedimentation. This gradual sedimentary-change interval with varying thickness might be the reason why dating around the boundary yields different results; it is not clear which stratigraphic level represents the beginning of the compressional event.

Our preferred MDA for the top of Punta Barrosa Formation (TPBA sample) is 85.5 ± 2.5 Ma and, the one taken from the first beds of Cerro Toro formation (CAS 63) is 87 ± 2 Ma. Both ages have been taken from the weighted average of the youngest cluster (Fig. 4). Both samples were taken from turbiditic sandstones and, although the sample taken in a stratigraphically higher position marks an older age, taking into account the uncertainties of each result, their error bar overlaps and allow us to estimate a ~87 Ma age for the transitional contact between formations.

The TCAS sample was taken from a turbiditic sandstone located just below the Lago Sofia conglomerate. For the MDA estimation we chose the weighted average of a 5 zircons group, which yielded in 83 ± 2 Ma (Fig. 4), a value close to the 83 Ma obtained by Bernhardt *et al.* (2012) (measured both in detrital and volcanic ash zircons) for the development of these submarine channels. Our results indicate a significant increase in sedimentation rate between the Punta Barrosa Formation (~35 m/Myr) and the fine-grain section of the Cerro Toro Formation (~175m/Myr).

The onset of the deposition of the Tres Pasos Formation in the study area was dated at 80 ± 2 Ma by Romans *et al.* (2010) using detrital zircons. Subsequently, Daniel *et al.* (2018) obtained a more precise 80.5 ± 0.3 Ma MDA for this boundary, based on volcanic ash zircons and 70.6 ± 1.5 Ma for the base of Dorotea formation with detrital zircons. We obtain an MDA of 75.0 ± 1.5 Ma (B3P sample) for the lower section of Tres Pasos Formation, near the Figueroa stratigraphic surface defined by Hubbard *et al.* (2010) and a MDA of 79 ± 9 Ma (A222 sample) in a similar stratigraphic level ~20 km to the south, both estimations based on the weighted average of the youngest zircon cluster (Fig. 4). In B3P the youngest single zircon was not taken into account in order to obtain a larger cluster for a better statistical value.

The hiatus related to the regional low-angle Paleogene unconformity increases northward: the longest documented non depositional or erosional interval occurs near Lago Viedma (~220 km to the north of the study area) where the Cangrejo Sandstone with an MDA of 18.1 ± 0.32 Ma overlays Upper Cretaceous Pari Aike Formation (Sickmann *et al.* 2018). At Río de las Chinas Valley (~85 km to the north of the study area), the hiatus decreases to ~20Myr, spanning from 65-63 Ma, which is the age of the Dorotea Formation to 45-40 Ma, the latter taken from the Man-Aike Formation (George *et al.* 2020). Closest measurements of the hiatus associated to the unconformity were taken ~30 km to the north of Rio Turbio Locality where it decreases to ~14 Myr from, spanning from ~60 to 46Ma (Fosdick *et al.* 2015a and 2020). Depositional ages obtained in this work were not robust enough to determine the precise chronology of the hiatus, which is probably due to the fact that the arc magmatic quiescence recorded between 60 and 45Ma (George *et al.* 2020) implies a lower supply of detrital zircons into the basin. Despite this uncertainty, the youngest zircon found in the upper levels of the Cerro Dorotea Formation (53.1 ± 1.3Ma) could indicate a strong decrease in the magnitude of the unconformity for those latitudes, constraining the hiatus to 10 Myr or less.

For the base of the Río Turbio Formation, we obtain a MDA of 51 ± 1 Ma using the youngest single zircon of BRTU sample and 47.0 ± 1.5 Ma from A220 sample with the same method (Fig. 4). Neither of them are statistically robust MDAs but the second one is consistent with previous studies that yield MDAs between ~47 and 45 Ma for the unit base (Fosdick *et al.* 2020; George *et al.* 2020). As in the sample from Cerro Dorotea Formation, the lack of arc magmatism between 60 and 45 Ma hinders obtaining precise depositional ages. Instead, the second sample of Rio Turbio Formation (FRTU), yielded a cluster of 3 zircons with lower Eocene ages that allows us to obtain a better MDA of 41 ± 3 Ma for this level (Fig. 4). The Rio Turbio Formation samples were taken from coarser sandstones then the older ones from this study and correspond to a shallower marine environment.

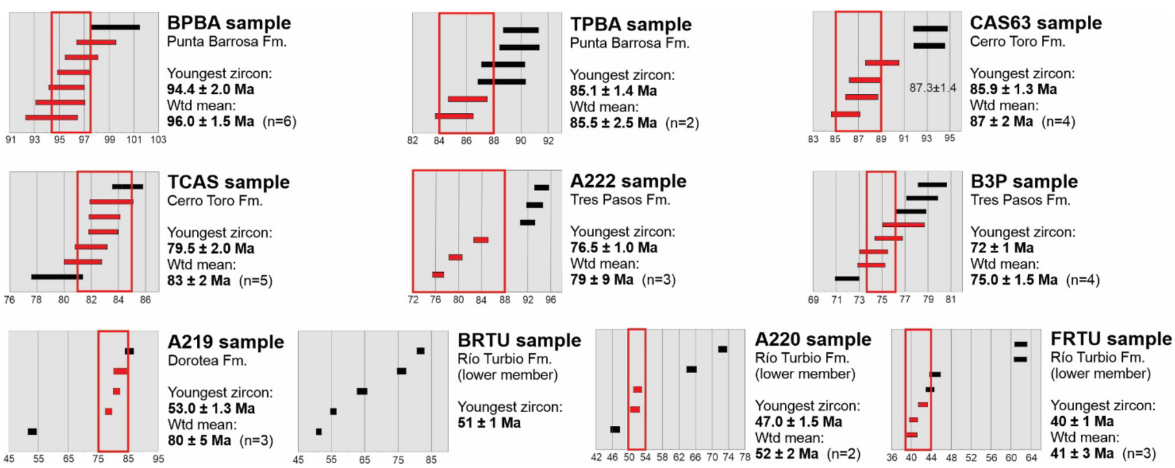

Figure 4. Detrital zircon U-Pb geochronological results: youngest zircons of each sample with 1σ uncertainties. Red rectangles indicate the zircon groups used for the MDA estimation.

BALANCED FORWARD MODELING

Structural modelling of the eastern Internal Domain and the Frontal Monocline

From fieldwork and satellite images a geologic map was drafted (Fig. 3) and locations for structural cross-sections chosen (Fig. 5). Fieldwork comprised identification of stratigraphic boundaries, fault traces, fold axes, and numerous bedding strike and dip measurements. Data was contrasted with previous papers including stratigraphic profiles, geologic / structural maps and seismic-reflection data (Wilson 1991; Malumián *et al.* 2000; Fildani and Hessler 2005; Ghiglione *et al.* 2009 y 2014; Hubbard *et al.* 2010; Fosdick *et al.* 2011; Romans *et al.* 2011; Bernhardt *et al.* 2012; Giacosa *et al.* 2012). Google Earth® and ESRI® base maps and satellite images were also used to create more accurate adjustments of outcrop boundaries, continuity of structural lineaments, and lithological changes. The projected topography in the cross-section is a single elevational transect taken from the ALOS PALSAR satellite radar, accessed through the Alaska Satellite Facility, which provides a digital elevation model of 12.5 m resolution. We performed forward structural modeling using the software Move from Petroleum Experts with its 2D modeling module. A cross-section of the fold-thrust belt was chosen, representative of the major structures of the study area oriented perpendicular to the mean bedding strike data. Nearby formational contacts, bedding geometries, faults and folds were projected onto the cross section.

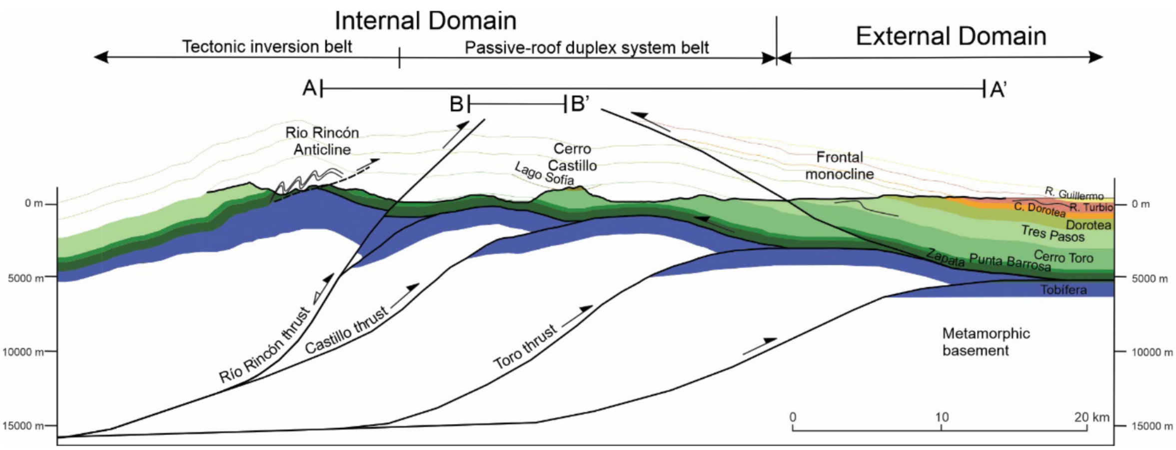

Figure 5. Structural cross-section A-A'across the fold-thrust belt along ~51°20'S latitude (see Fig. 3 for location).

Description of the cross section

Along the section, three belts were identified with contrasting structural features, such as the magnitude of internal deformation (minor scale faults and folds) and the age of the outcropping units, allowing us to assume that the deformational mechanisms might have been different. Those belts are:

i) Río Rincón thrust and anticline

The mountain range known as Cordillera Arturo Prat is located on the western boundary of the study area depicting the highest topography, with peaks reaching up to 1590 m a.s.l. at Cerro Tenerife. These ranges expose Jurassic synrift deposits, the entire section of the Lower Cretaceous Zapata Formation and parts of the lower Punta Barrosa Formation. It emerges as a large anticline known as Rio El Rincón anticline (Wilson 1983, 1991, Fosdick *et al.* 2011). The structural model that best fits the geometry of these deformed outcrops, involving uplift and folding of Jurassic rocks, corresponds to a fault propagation fold where the original west-dipping fault is modelled with an angle of ~60°. For this structure and the duplex system structure to be explained below we concur with a depth of detachment at ~15 km within the Paleozoic metamorphic basement, as identified by seismic data and used in previous structural interpretations (Harambour 2002; Fosdick *et al.* 2011; Ghiglione *et al.* 2014). Within this major anticline, an intense thin-skinned deformation develops which includes tight folds and faults with detachment in the Zapata Formation known as the Tenerife thrust zone, described by Fosdick *et al.* (2011). Thus, Rio Rincón anticline accommodates a much higher magnitude of shortening in the Cretaceous sedimentary cover than in the basement and synrift deposits.

ii) Cerro Castillo – Cerro Toro duplex system

The central belt of the study area has a less elevated topography than the western one: its most important peaks are the Cerro Castillo and Cerro Mocho with ~1200 m.a.s.l. located in a mountain range called Cordillera Manuel Señoret. Folds observed in this belt are gentle and have longer wavelengths (tens of kilometers) than those belonging to the Cordillera Arturo Prat, reflecting a clear change in the deformation mechanism between those belts. Deformation mechanism that achieved the best fit in our model is a basement cored duplex system with an upper detachment level in the lower Zapata Formation. The eastern thrust sheet forms a passive roof duplex system leading to the frontal monocline development. The duplex was interpreted as a stack of 3 fault bend fold thrusts, exposed at the surface as the Cerro Castillo and Cerro Toro anticlines and the Frontal Monocline. South of the selected section, this belt seems to narrow and disappear while, towards the north the duplex system broadens apparently related with an increase in the number of thrust sheets (Fig. 3).

Although most recent structural models for the Patagonian fold-thrust belt propose the incorporation of the basement into the deformation using fault inversion as the main mechanism, there is evidence from seismic lines that indicate that not all basement faults are reactivated ones, especially on the eastern margin of the orogen (Fosdick *et al.* 2011; Giacosa *et al.* 2012; Ghiglione *et al.* 2014). Another possibility is that the Castillo and Toro thrust have an extensional origin but, at the time of inversion they have used short-cut mechanisms.

iii) Frontal monocline

The eastern belt is characterized by an extensive monocline sequence of ~25° eastward dipping shallowing to the east. Internally it contains some smaller-scale folds with shallower detachments (Fig. 5). In our proposed model, this structure is controlled by inception of the basement wedge described before and, on top, the generation of a backthrust that further tilts the Campanian to early Miocene strata and soles out in the base of the Zapata Formation, a level identified as mechanically weak by previous studies due to its mudstone composition and hydrocarbon content (Rojas and Mpodozis 2006; Klepeis *et al.* 2010; Fosdick *et al.* 2011; Betka *et al.* 2015).

Crustal deformation resulted in a total 20.3 km (20%) shortening. For the basement and synrift deposits, most of the shortening is concentrated in the duplex system (16.3 km) and a minor part in the Rio Rincon anticline (4 km). On the contrary, the sedimentary cover appears to concentrate shortening in minor scale faults and folds (schematically drawn in our model, Fig. 5) developed within the Rio Rincón anticline, where Fosdick *et al.* (2011) infers ~6.5 km shortening in this thin-skinned deformation. A similar decoupling effect causing an inhomogeneous shortening distribution between the basement and the Cretaceous sedimentary cover was described ~180 km to the south by Betka *et al.* (2015).

Exhumation ages

There are a number of previous studies that include exhumation ages for the study area and neighboring locations based on thermochronology and stratigraphy. Süssenberger *et al.* (2018) identify exhumation periods using K-Ar dating on synkinematically formed illite in low-grade metamorphic mudstones. They obtained ~58 Ma for the Río Rincón thrust and ~54 Ma for the associated anticline exhumed from beneath the closure-temperature isotherm (~300 °C), structures that we interpreted as a result of tectonic inversion of the Jurassic rift.

Another exhumation event is documented by Calderon *et al.* (2012) in the western margin of the orogen around ~85 Ma using $^{40}Ar/^{39}Ar$ age for the obduction of the Sarmiento Ophiolitic Complex. Close to that age, there was an increase in the incorporation of Upper Jurassic zircons to the basin, which could mean the exhumation and denudation of rift deposits (Romans *et al.* 2010; Malkowski *et al.* 2018). Although these thrust-related exhumation evidences correspond to locations west of the study area, there are some insights that the Lago Sofia member could be deposited in a wedge top context (Crane and Lowe 2008; Gonzales and Aydin 2008; Bernhardt *et al.* 2011; Ghiglione *et al.* 2014).

Zircon and apatite (U-Th)/He ages (Zhe and AHe) obtained by Fosdick *et al.* (2013) indicate widespread exhumation of the internal and external domain between 22 and 4 Ma. While the oldest ages of this period can be attributed to structural uplift processes, the youngest ones are associated with a strong denudation process produced by glaciations from 7 Ma onwards (Thomson *et al.* 2010; Fosdick *et al.* 2013). Thermochonology data from these reports support exhumation between 22 and 17 Ma ZHe and 6 Ma AHe (above the ~200°C and ~75°C isotherm, respectively) in the Río Rincón anticline and La Peninsula syncline (Fig. 3), which is significantly younger than the values obtained by Süssenberger *et al.* (2018) from illite analysis in similar positions. Fosdick *et al.* (2013) also obtained 44 to 42 Ma ZHe in samples taken from upper Cretaceous units in the Cerro Toro anticline (~15 km to the north of the study area), 8 Ma AHe in the Cerro Castillo and 10 Ma AHe in the Frontal Monocline.

Another relevant thermochronological study indicates a burial peak temperature between 164 °C and 180 °C for the Dorotea Formation during the early Eocene (54–46 Ma) followed by a rapid exhumation and erosion (Fosdick *et al.* 2015b). These burial magnitudes are inconsistent with vitrinite reflectance data that yield between ~70 and 100 °C of heating measure in similar stratigraphic levels (Ali 2016; George *et al.* 2020). Thermal modeling obtained by Ali (2016) combining Zircon (U-Th)/He and vitrinite reflectance data in our study area indicates a rapid heating between ~62 and 55 Ma followed by cooling between ~55 and 47 Ma, again heating between ~47 and 14 Ma at a slower speed and temperature than before, and finally cooling from 14 Ma onwards.

There are some features of the Cenozoic stratigraphic record that can be interpreted as a response to tectonic uplift processes and match in time with thermochronological exhumation data, those are: (1) the basin-wide Paleogene unconformity with a ~15 Myr (or shorter) hiatus at the study latitude. (2) Unconformities within Río Turbio Formation: the unit is composed by two members that seems to have one hiatus according to U-Pb geochronological (between ~40 to ~36 Ma) and biostratigraphic data. Another possibility indicates that it is not a single unconformity but a series of progressive unconformities (Malumian *et al.* 2000; Fosdick *et al.* 2015a, 2020). (3) Late Oligocene- Early Miocene unconformity between Rio Turbio and Rio Guillermo Formation. Bridging a hiatus of ~2 Ma, it separates deposits belonging to very different depositional environments: from shallow marine (below) to fully continental coarse-grained fluvial deposits (above) (Fosdick *et al.* 2020; Leonard *et al.* 2020).

DISCUSSION

Early compressional stages: onset of foreland basin and tectonic inversion

The appearance of sandy turbidites with Andean provenance covering hypabyssal mudstone deposits in the basin is considered as evidence of the onset of a compressional stage (Wilson 1991; Fildani *et al.* 2003; Romans *et al.* 2011). This change in tectonic dynamics started in Aptian-Albian time in the northwestern part of the basin causing diachronous closure from north to south (Malkowski *et al.* 2015; Aramendía *et al.* 2018; Ronda *et al.* 2019; Barberón *et al.* 2019). Those turbidite depositional systems were dated at ~115 Ma at Lago Viedma latitude (Malkowski *et al.* 2015), between ~101 and 92 Ma at Lago del Toro latitude (Fildani *et al.* 2003; Fosdick *et al.* 2011; Daniels *et al.* 2019, this study) and ~89 Ma ~250 km further south (McAtamney *et al.* 2011).

A decrease in thickness and grain size of sandstone beds of turbiditic origin marks the beginning of Cerro Toro Formation at ~87 Ma. MDA results indicate a much higher sedimentation rate for this unit than for the underlying Punta Barrosa Formation. Detrital zircon age distributions for this unit show a change in the sediment source area, with the appearance of clastices derived from sources related to extensional volcanism to the west, i.e. Sarmiento Ophiolitic Complex and Tobífera Formation (Romans *et al.* 2010; Malkowski *et al.* 2018). These change in input data are consistent with uplift studies of both units along the Canal de las Montañas shear zone and the Tobífera Duplex (Calderón *et al.* 2012; Fosdick *et al.* 2011). In the context of intense deformation in the basement domain from Santonian/Campanian time, we believe that the advance of the orogenic front at the study latitude reached the Río Rincón thrust, inverting an originally normal fault. The deposits of the main turbidite channel belt known as Lago Sofia conglomerates (MDA of ~83 Ma) currently lie ~10 km eastward of the Rio Rincon thrust maintaining paleocurrents directions parallel to the fault trace (Figs. 3 and 6). We propose that this channel developed in a proximal foredeep context where the orogenic front is represented by the Rio Rincón anticline in its early uplift stages (Fig. 6). The same pattern is observed with the Rio Nutria thrust and the Silla Syncline tributary channel ~25 km to the north of the study area where similar interpretations have been made (Crane and Lowe 2008; Gonzales and Aydin 2008; Bernhardt *et al.* 2011).

Paleocene - Eocene exhumation

The origin and timing of the Cerro Dorotea - Río Turbio unconformity is still a matter of debate. In the study area is difficult to arrive to precise depositional ages using detrital zircons due to the absence of arc volcanism during this time span. Recent studies based on detrital zircons indicate a ~60 to 46 Ma hiatus and, although the youngest zircon found in the upper Cerro Dorotea Formation in our sampling is ~53 Ma, currently it does not have enough statistical weight to assert that the unit reaches Eocene ages (Fig. 4).

The thickness of the eroded column during this hiatus is also uncertain, with large discrepancies in the thermochronological results. For our model we use the measurements of Ali (2016) which combines zircon (U-Th)/He and vitrinite reflectance data concluding that Cerro Dorotea Formation experienced burial heating between ~62 and 54 Ma followed by slow cooling and exhumation with loss of ~720 m of the sedimentary column (Fig. 6), and cooling lasting until ~47 Ma. The wide geographical extension over which the unconformity has been recorded and the very low angularity makes it plausible to consider it related to regional uplift rather than a result of localized thrusting (Fig. 6).

The first signs of Cenozoic thrusting (Fig. 6) are the ~42 and 44 Ma ZHE in the Toro Anticline (Fosdick *et al.* 2013), contemporaneous with the development of unconformities within Río Turbio Formation and the changes in zircon provenance from Eocene onward (Fosdick *et al.* 2020).

Miocene exhumation

In contrast to Paleocene-Eocene time, exhumation events taking place during Late Oligocene and Miocene time appear to be much clearer and better documented. ZHE and AHE values indicate a generalized uplift of the internal fold-thrust belt starting at 22 Ma. In the study area, Río Guillermo Formation lies unconformably on the Río Turbio Formation. Recent MDA data show ages for the base of Rio Guillermo Formation between 26 and 24 Ma (Fig. 7) which could be evidence that uplift began before than 22 Ma. However, estimation on eroded sedimentary

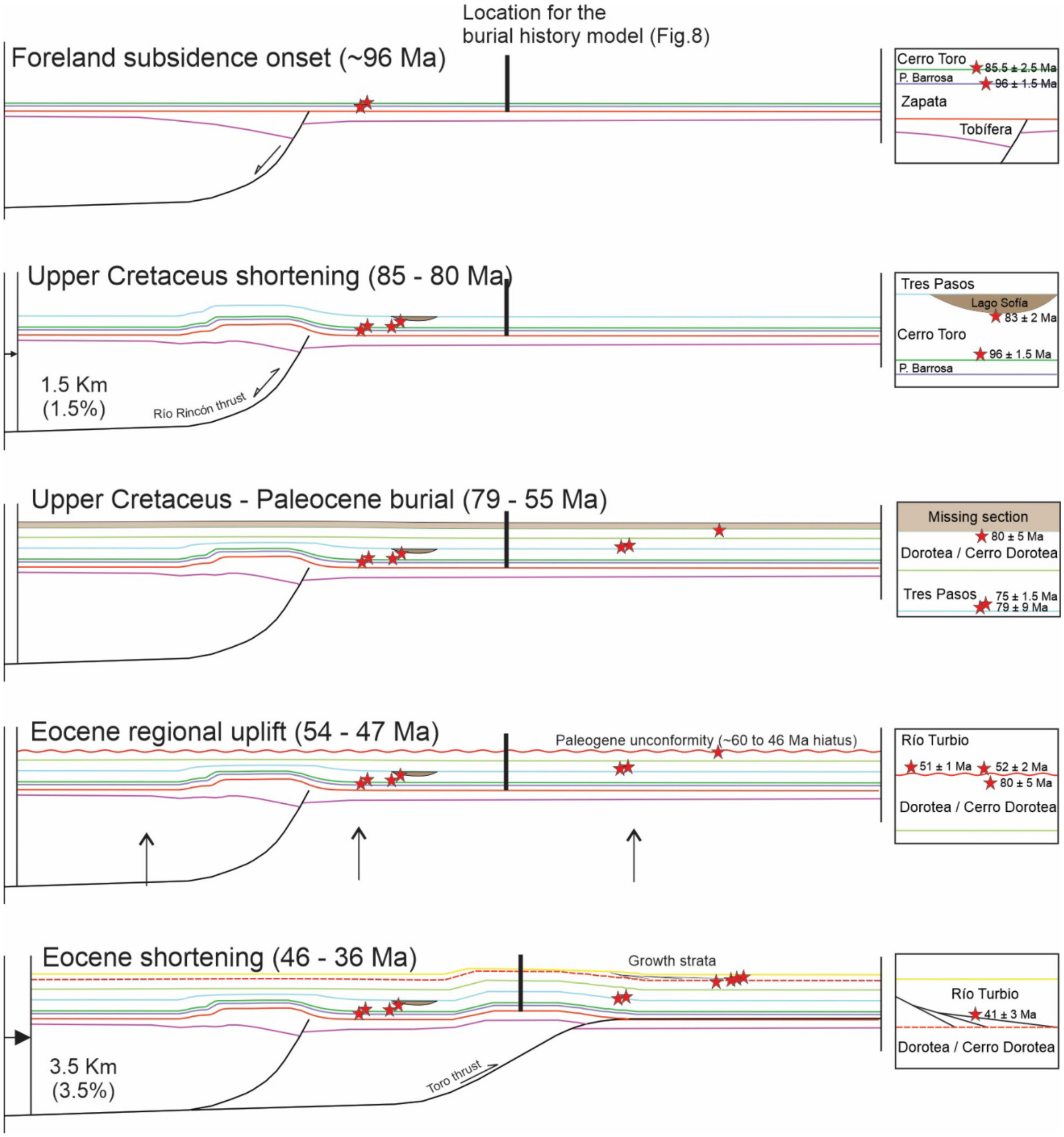

Figure 6. Kinematic-structural model of the orogenic front with Cretaceous to Paleogene tectonic events. Red stars indicate the detrital zircon sample locations. The boxes on the right side of the figure show the stratigraphic units that are incorporated into the structural cross-section for each step and the MDAs obtained in this study. Two shortening episodes are represented for this timeframe, one in the Upper Cretaceous and the other in the Eocene time.

thickness is comparatively low: ~30m (Ali 2016).

In our model we propose an uplift of the internal domain and frontal monocline, where most of the shortening occurs during Miocene time: starting with the reactivation of originally extensional faults, followed by a basement duplex system development and finally a generation of low-angle thrust and backthrust (Fig. 7). From Pliocene time onwards, exhumation continues but more related to erosional glaciation processes than to the effects of crustal shortening (Fig. 7).

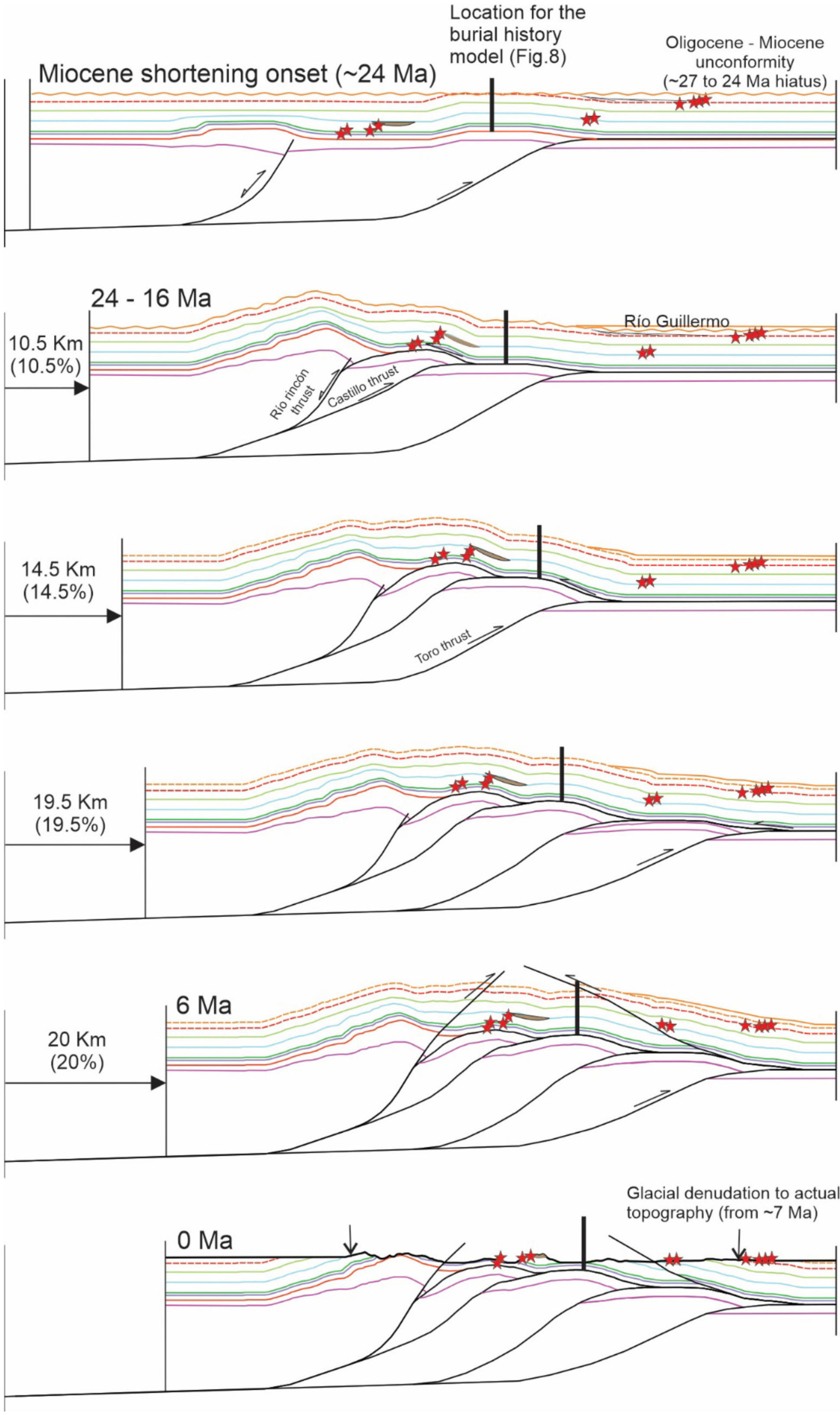

Figure 7. Kinematic-structural model of the orogenic front from Miocene to actual time. Most of the shortening occurs during Miocene time, reaching 20 km (20%).

1-D burial history and maturity zones

We use the Petromod software to made one-dimensional (1D) burial and maturity history models (Fig. 8).

Unit thicknesses and compile geochronological data presented in this work provides an excellent input for those models. In addition, we count with thermochronological data from the study area that allows us to estimate the possible eroded thicknesses during the development of unconformities as we discussed in the previous sections of this work. The model also requires two boundary conditions which are: the paleo heat flow of the area during the modeled timeframe and the paleo water depth during deposition. Paleo heat flow of the western margin of the austral basin were taken from Sachse *et al.* (2016b) and paleo water depths were taken from Natland *et al.* (1974), Schwartz and Graham (2015) and Schwartz *et al.* (2016).

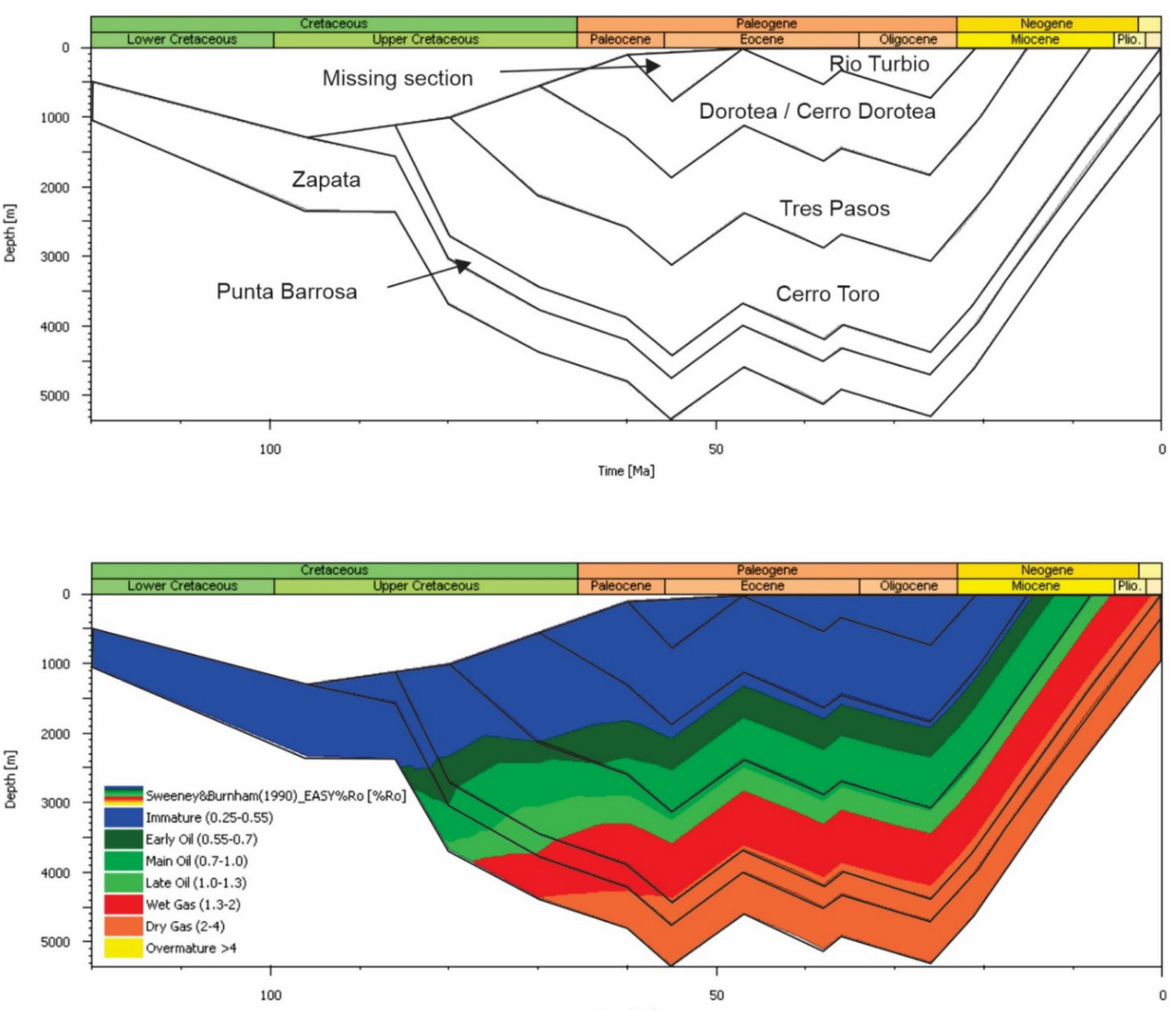

Figure 8. Burial history curves with maturity zones (determined from the EASY %Ro method: Sweeney and Burnham 1990).

We chose to represent in the model the evolution of the Toro anticline (Figs. 6 and 7, black stick) because it is a very representative structure of the area in terms of its scale and northward continuity, and because of its central position in relation to the zircon sample locations and thickness measurements.

The results of the burial model show a marked acceleration of the sedimentation rate for the Campanian Time (during the deposition of the Cerro Toro Formation). Burial continued until ~55 Ma where Cretaceous units reach a maximum above 5000 m depth for the bottom of Zapata formation. Two uplift processes are represented in the model for the Eocene time followed by the major uplift stage beginning towards late Oligocene time and reaching ~4000 m of eroded thickness.

The maturity zones were determined from the EASY %Ro method of Sweeney and Burnham (1990). For the Zapata formation (Lower Palermo Aike, the main source rock of the basin), the early oil window was reached at depths of ~2500 m at ~85 Ma while the main oil window was reached ~2 Myr later. Wet gas window for the same unit was reached at 3800 m at ~76 Ma. The dry gas window is the maximum degree of maturity of the unit. Another feature that appears from the model is the maturity that would be expected for the shale-rich Cerro Toro and Tres Pasos Formation. For the first one, we would expect a Ro% between 2.1 and 1, while for the second one the expected Ro% would be between 1 and 0.5.

CONCLUSIONS

In the Ultima Esperanza area, onset of compression dates back to the Cenomanian (96.0 ± 1.5 Ma, our data) and remained active until Campanian time. From Campanian to Danian times, sedimentary infill was marked by a shallowing upwards trend. Late Paleocene and Eocene events are still not entirely clear; while the sedimentary record presents an unconformity with a hiatus of at least 10 Myr, evidences of fault activation for that period are inconclusive. Our working hypothesis is that this exhumation stage would respond mostly to dynamic uplift processes associated with the passage of the Farallon-Aluk ridge. Major crustal shortening began in the Late Oligocene-Early Miocene time, recorded by another unconformity persisting during the whole Miocene. We estimated a total (20%) shortening distributed differently in two decoupled lithostratigraphic units: basement and synrift deposits present greater shortening in a duplex system that soles out ~15 km depth while the Cretaceous sedimentary column accumulates higher shortening in smaller scale structures within the Río Rincón anticline with a detachment in a weak level of Zapata Formation.

From the burial and maturity model we obtain that the oil and gas generation window for the main source rock was reached between the Campanian and Maastrichtian time and the highest degree of maturity at Paleogene-early Eocene time.

ACKNOWLEDGEMENTS

This work has been carried out with financial support from YPF S.A., and CONICET PIP 11220200100307CO, UBACYT and PICT-2020-SERIEA-03277 to MG. We thank Inés Aramendía and Vanesa Barberón for field assistance and Mauricio Calderón and Paulo Quesada for the constructive and inspiring discussions. We also thank José Rivera from the Estancia Complejo Torres del Paine who always received us friendly and granted access to the outcrops.

REFERENCES

Aguirre Urreta, M.B., 2002. Invertebrados del Cretácico inferior. In: Haller, M. J. (Ed.), Geología y Recursos Naturales de Santa Cruz. Relatorio XV Congreso Geológico Argentino, pp. 439-459.

Ali, R.A., 2016. Paleogene tectonic and thermal evolution of the Magallanes Basin, Chile, 50°30'-51°30'S: A study using zircon (U-Th)/He thermochronology and vitrinite reflectance [M.S. Thesis]: Indiana University, 96 p.

Arbe H.A., 2002. Análisis estratigráfico del Cretácico de la Cuenca Austral. In Haller MJ (ed) Geología y Recursos Naturales de Santa Cruz. Relatorio del XV Congreso Geológico Argentino, pp 103–128

Aramendía, I., Ramos, M.E., Geuna, S., Cuitiño, J.I., and Ghiglione, M.C., 2018. A multidisciplinary study of the Lower Cretaceous marine to continental transition in the northern Austral-Magallanes basin and its geodynamic significance. Journal of South American Earth Sciences, 86, 54-69.

Armitage, D.A., Romans, B.W., Covault, J. A., and Graham, S.A., 2009. The influence of mass-transport-deposit surface topography on the evolution of turbidite architecture: The Sierra Contreras, Tres Pasos Formation (Cretaceous), southern Chile. Journal of Sedimentary Research, 79(5), 287-301.

Barberón, V., Ronda, G., Aramendía, I., Suárez, R.J., Ramos, M.E., Naipauer, M., Sue, C., and Ghiglione, M. C., 2019. Tectonic evolution of the northern Austral-Magallanes basin in the Southern Patagonian Andes from provenance analysis. Journal of South American Earth Sciences, 95, 102234.

Bernhardt, A., Jobe, Z.R. and Lowe, D.R., 2011. Stratigraphic evolution of a submarine channel-lobe complex system in a narrow fairway within the Magallanes foreland basin, Cerro Toro Formation, southern Chile Marine and Petroleum Geology. 28, 785–806. https://doi.org/10.1016/j.marpetgeo.2010.05.013.

Bernhardt, A., Jobe, Z.R., Grove, M. and Lowe, D.R., 2012. Palaeogeography and diachronous infill of an ancient deep-marine foreland basin, Upper Cretaceous Cerro Toro Formation. Magallanes Basin. Basin Research. 24, 269–294. https://doi.org/10.1111/j. 1365-2117.2011.00528.x.

Betka, P., Klepeis, K., and Mosher, S., 2015. Along-strike variation in crustal shortening and kinematic evolution of the base of a retroarc fold-and-thrust belt: Magallanes, Chile 53° S–54° S. Bulletin, 127(7-8), 1108-1134.

Calderón, M., Fosdick, J.C., Warren, C., Massonne, H.-J., Fanning, C.M., Fadel Cury, L., Schwanethal, J., Fonseca, P.E., Galaz, G., Gaytan, D. and Herve, F., 2012. The low-grade Canal de las Montanas Shear Zone and its role on the tectonic emplacement of the Sarmiento Ophiolitic Complex and Late Cretaceous Patagonian Andes orogeny, Chile. Tectonophysics 524–525, 165–185. https://doi.org/10.1016/j.tecto.2011.12.034.

Calderón, M., Fildani, A., Hervé, F., Fanning, C.M., Weislogel, A. and Cordani, U., 2007. Late Jurassic bimodal magmatism in the northern sea-floor remnant of the Rocas Verdes basin, southern Patagonian Andes. Journal of the Geological Society. 164:1011–1022

Calderón, M., Hervé, F., Fuentes, F., Fosdick, J. C., Sepúlveda, F., and Galaz, G., 2016. Tectonic evolution of Paleozoic and Mesozoic andean metamorphic complexes and the Rocas Verdes ophiolites in southern Patagonia. In Geodynamic Evolution of the Southernmost Andes (pp. 7-36). Springer, Cham.

Cecioni, G.O., 1957. Cretaceous flysch and molasses in departamento Ultima Esperanza, Magallanes Province, Chile. AAPG Bulletin. 41, 538–564.

Covault, J.A., Romans, B.W. and Graham, S.A., 2009. Outcrop expression of a continentalmargin-scale shelf-edge delta from the Cretaceous Magallanes Basin, Chile. J. Sediment. Research. 79, 523–539. https://doi.org/10.2110/jsr.2009.053.

Crane, W.H. and Lowe, D.R., 2008. Architecture and evolution of the paine channel complex, Cerro Toro Formation (upper Cretaceous), Silla Syncline, Magallanes basin, Chile. Sedimentology 55, 979–1009. https://doi.org/10.1111/j.1365-3091.2007.00933.x.

Dalziel, I.W.D., 1981. Back-arc extension in the southern Andes: a review and critical reappraisal. Philosophical Transactions of the Royal Society of London. Series A, Mathematical and Physical Sciences, 300(1454), 319-335.

Daniels, B.G., Auchter, N.C., Hubbard, S.M., Romans, B.W., Matthews, W.A. and Stright, L., 2018. Timing of deep-water slope evolution constrained by large-n detrital and volcanic ash zircon geochronology, Cretaceous Magallanes Basin, Chile. GSA Bulletin. 130, 438–454. https://doi.org/10.1130/B31757.1.

Daniels, B.G., Hubbard, S.M., Romans, B.W., Malkowski, M.A., Matthews, W.A., Bernhardt, A., Kaempfe, S.A., Jobe, Z.R., Fosdick, J.C., Schwartz, T.M., Fildani, A., Graham, S.A., 2019. Revised chronostratigraphic framework for the Cretaceous Magallanes-Austral Basin, Última Esperanza Province, Chile: Journal of South American Earth Sciences. 94, 102209 https://doi.org/10.1016/j.jsames.2019.05.025

Dickinson, W.R., and Gehrels, G.E., 2009. Use of U–Pb ages of detrital zircons to infer maximum depositional ages of strata: a test against a Colorado Plateau Mesozoic database. Earth and Planetary Science Letters, 288(1-2), 115-125.

Feruglio, E., 1938. Relaciones estratigráficas entre el Patagoniano y el Santacruciano en la Patagonia Austral. Revista del Museo de La Plata, 1(4), 129-159.

Fildani, A. and Hessler, A.M., 2005. Stratigraphic record across a retroarc basin inversion: Rocas Verdes–Magallanes basin, Patagonian Andes. GSA Bulletin. 117, 1596–1614. https://doi.org/10.1130/B25708.1.

Fildani, A., Cope, T.D., Graham, S.A. and Wooden, J.L., 2003. Initiation of the Magallanes foreland basin: timing of the southernmost Patagonian Andes orogeny revised by detrital zircon provenance analysis. Geology 31, 1081–1084. https://doi.org/10.1130/G20016.1.

Fosdick, J.C., Romans, B.W., Fildani, A., Bernhardt, A., Calderon, M. and Graham, S.A., 2011. Kinematic evolution of the Patagonian retro-arc fold-and-thrust belt and Magallanes foreland basin, Chile and Argentina, 51°30'S. GSA Bulletin. 123, 1679–1698. https://doi.org/10.1130/B30242.1.

Fosdick, J.C., Grove, M., Hourigan, J.K. and Calderón, M., 2013. Retroarc deformation and exhumation near the end of the Andes, southern Patagonia. Earth and Planetary Science Letters. 361, 504–517. https://doi.org/10.1016/j.epsl.2012.12.007.

Fosdick, J. C., Bostelmann, J. E., Leonard, J., Ugalde, R., Oyarzún, J. L., and Griffin, M., 2015a. Timing and rates of foreland sedimentation: New detrital zircon U/Pb geochronology of the Cerro Dorotea, Río Turbio, and Río Guillermo formations, Magallanes basin. In XIV Congreso Geológico Chileno (pp. 152-166).

Fosdick, J.C., Grove, M., Graham, S.A., Hourigan, J.K., Lovera, O. and Romans, B.W., 2015b. Detrital thermochronologic record of burial heating and sediment recycling in the Magallanes foreland basin, Patagonian Andes. Basin Research. 27, 546–572. https://doi.org/10.1111/bre.12088.

Fosdick, J. C., VanderLeest, R. A., Bostelmann, J. E., Leonard, J. S., Ugalde, R., Oyarzún, J. L., and Simms, A. R., 2020. Revised timing of Cenozoic Atlantic incursions and changing hinterland sediment sources during southern Patagonian orogenesis. Lithosphere, 2020(1).

George, S.W., Davis, S.N., Fernández, R.A., Manríquez, L.M., Leppe, M.A., Horton, B.K., and Clarke, J.A., 2020. Chronology of deposition and unconformity development across the Cretaceous–Paleogene boundary, Magallanes-Austral Basin, Patagonian Andes. Journal of South American Earth Sciences, 97,102237.

Ghiglione, M.C., Suárez, F., Ambrosio, A., Da Poian, G., Cristallini, E.O., Pizzio, M.F. and Reinoso, R.M., 2009. Structure and evolution of the Austral basin fold–thrust belt, southern Patagonian Andes. Revista de la Asociación Geológica Argentina 65:215–226

Ghiglione, M.C., Likerman, J., Barberon, V., Beatriz Giambiagi, L., Aguirre-Urreta, B. and Suarez, F., 2014. Geodynamic context for the deposition of coarse-grained deepwater axial channel systems in the Patagonian Andes. Basin Research. 26, 726–745 10.1111/bre.12061.

Giacosa, R., Fracchia, D. and Heredia, N., 2012. Structure of the Southern Patagonian Andes at 49°S, Argentina. Geologica Acta 10 (3), 265-282.

Gonzales, J., & Aydin, A., 2008. Structural characterization of deep-water deposits in a foreland basin, Silla Syncline (Chilean Patagonia), with applications to depositional processes. Journal of Structural Geology, 30(9), 1095-1108.

Harambour, S.M., and Haller, M.J., 2002. Deep-seated thrusts in the frontal part of the Magallanes fold and thrust belt, Ultima Esperanza, Chile. In XV Congreso Geológico Argentino (Vol. 3, p. 230). El Calafate Argentina.

Herve, F., Fanning, C.M., and Pankhurst, R.J., 2003. Detrital zircon age patterns and provenance of the metamorphic complexes of southern Chile. Journal of South American Earth Sciences, 16(1), 107-123.

Hubbard, S.M., Romans, B.W. and Graham, S.A., 2008. Deep-water foreland basin deposits of the Cerro Toro Formation, Magallanes Basin, Chile: architectural elements of a sinuous basin axial channel belt. Sedimentology 55, 1333–1359. https://doi.org/10.1111/j.1365-3091.2007.00948.x.

Hubbard, S.M., Fildani, A., Romans, B.W., Covault, J.A. and McHargue, T.R., 2010. Highrelief slope clinoform development: insights from outcrop, Magallanes Basin, Chile. Journal of Sedimentary Research, 80, 357–375. https://doi.org/10.2110/jsr.2010.042.

Hünicken, M., 1955. Depósitos neocretácicos y terciários del extremo ssw de Santa Cruz: cuenca carbonífera de Río Rurbio (Vol. 4, No. 1). Instituto Naciobal de Investigacion de las Ciencias Naturales.

Jobe, Z.R., Bernhardt, A. and Lowe, D.R., 2010. Facies and architectural asymmetry in a conglomerate-rich submarine channel fill, Cerro Toro Formation, Sierra del Toro, Magallanes, Chile. Journal of Sedimentary Research. 80, 1085–1108. https://doi.org/10.2110/jsr.2010.092.

Katz, H.R., 1963. Revision of Cretaceous stratigraphy in Patagonian cordillera of Ultima Esperanza, Magallanes Province, Chile. AAPG Bulletin. 47, 506–524.

Klepeis, K., Betka, P., Clarke, G., Fanning, M., Hervé, F., Rojas, L., Mpodozis, C., and Thomson, S., 2010. Continental underthrusting and obduction during the Cretaceous closure of the Rocas Verdes rift basin, Cordillera Darwin, Patagonian Andes. Tectonics, 29(3).

Leanza, A.F., 1972. Andes Patagónicos Australes. Geología Regional Argentina, Academia Nacional de Ciencias, Córdoba, pp 689–706

Leonard, J.S., Fosdick, J.C., and VanderLeest, R.A., 2020. Erosional and tectonic evolution of a retroarc orogenic wedge as revealed by sedimentary provenance: case of the Oligocene–Miocene Patagonian Andes. Frontiers in Earth Science, 7, 353.

Likerman, J., Burlando, J.F., Cristallini, E.O., and Ghiglione, M.C., 2013. Along-strike structural variations in the Southern Patagonian Andes: insights from physical modeling. Tectonophysics, 590, 106-120.

Ludwig, K.R., 2003. Isoplot 3.00: A geochronological toolkit for Microsoft Excel. Berkeley Geochronology Center Special Publication, 4, 70.

Macellari, C.E., Barrio, C.A. and Manassero, M.J., 1989. Upper Cretaceous to Paleocene depositional sequences and sandstone petrography of southwestern Patagonia (Argentina and Chile). Journal of South American Earth Science 2: 223-239.

Malkowski, M.A., Sharman, G.R., Graham, S.A. and Fildani, A., 2015. Characterisation and diachronous initiation of coarse clastic deposition in the Magallanes-Austral foreland basin, Patagonian Andes. Basin Research. 29, 298–326. https://doi.org/10.1111/bre.12150.

Malkowski, M.A., Grove, M. and Graham, S.A., 2016. Unzipping the Patagonian Andes – long lived influence of rifting history on foreland basin evolution. Lithosphere 8, 23–28.https://doi.org/10.1130/L489.1.

Malkowski, M.A., Jobe, Z.R., Sharman and G.R. and Graham, S.A., 2018. Down-slope facies variability within deep-water channel systems: insights from the Upper Cretaceous Cerro Toro Formation, southern Patagonian. Sedimentology 65, 1918–1946. https://doi.org/10.1111/sed.12452.

Malumián, N. and Caramés, A., 1997. Upper Campanian-Paleogene from the Río Turbio coal measures in southern Argentina: Micropaleontology and the Paleocene/Eocene boundary Journal of South American Earth Sciences 10:189–201

Malumian, N. and Nanez, C., 2011. The Late Cretaceous–Cenozoic transgressions in Patagonia and the Fuegian Andes: foraminifera, palaeoecology, and palaeogeography. Biological Journal of the Linnean Society, 103(2), 269-288.

Malumián, N., Panza, J.L.A. and Parisi, C., 2000. Hoja geológica 5172-III Yacimiento Río Turbio.

McAtamney, J., Klepeis, K., Mehrtens, C., Thomson, S., Betka, P., Rojas, L. and Snyder, S., 2011. Along-strike variability variability of back-arc basin collapse and the initiation of sedimentation in the Magallanes foreland basin, southernmost Andes (53-54.5°S). Tectonics 30, TC5001. https://doi.org/10.1029/2010TC002826.

Mpodozis, C., and Ramos, V., 1990. The Andes of Chile and Argentina.

Natland, M. L., 1974. A system of stages for correlation of Magallanes Basin sediments (Vol. 139). Geological Society of America.

Pankhurst, R.J. and Rapela, C.W., 1995. Production of Jurassic rhyolite by anatexis of the lower crust of Patagonia. Earth and Planetary Science Letters 134: 23-26, Amsterdam.

Pankhurst, R.J., Riley, T.R., Fanning, C.M. and Kelley, S.P., 2000. Episodic silicic volcanism in Patagonia and Antarctic Peninsula: chronology of magmatism associated with the break-up of Gondwana. Journal of Petrology. 41, 605–625. https://doi.org/10.1093/petrology/41.5.605.

Riccardi, A.C. and Rolleri, E.O., 1980. Cordillera Patagonica Austral. Actas Segundo Simposio de Geologia Regional Argentina 2, 1173–1306.

Rojas, L., and Mpodozis, C., 2006. Geología estructural de la Faja Plegada y Corrida del sector chileno de Tierra del Fuego, Andes patagónicos australes. In Congreso Geológico Chileno (No. 11, pp. 325-328).

Romans, B.W., Fildani, A., Graham, S.A., Hubbard, S.M.and Covault, J.A., 2010. Importance of predecessor basin history on the sedimentary fill of a retroarc foreland basin: provenance analysis of the Cretaceous Magallanes basin, Chile (50-52°S). Basin Research. 22, 640–658. https://doi.org/10.1111/j.1365-2117.2009.00443.x.

Romans, B.W., Fildani, A., Hubbard, S.M., Covault, J.A., Fosdick, J.C. and Graham, S.A., 2011. Evolution of deep-water stratigraphic architecture, Magallanes Basin, Chile. Marine and Petroleum Geology 28, 612–628. https://doi.org/10.1016/j.marpetgeo.2010.05.002.

Ronda, G., Ghiglione, M.C., Barberón, V., Coutand, I., and Tobal, J., 2019. Mesozoic–Cenozoic evolution of the Southern Patagonian Andes fold and thrust belt (47°–48° S): Influence of the Rocas Verdes basin inversion and onset of Patagonian glaciations. Tectonophysics, 765, 83-101.

Russo, A., Flores, M.A. and Di Benedetto, H., 1980. Patagonia Austral Extraandina. II Simposio de Geología Regional Argentina, Actas 2:1431–1462

Sachse, V.F., Strozyk, F., Anka, Z., Rodriguez J.F. and di Primio, R., 2016a. The tectono-stratigraphic evolution of the Austral Basin and adjacent areas against the background of Andean tectonics, southern Argentina,South America. Basin Research 28, 462-482.

Sachse, V. F., Anka, Z., Littke, R., Rodriguez, J. F., Horsfield, B., and di Primio, R., 2016b. Burial, temperature and maturation history of the Austral and western Malvinas basins, southern Argentina, based on 3D basin modelling. Journal of Petroleum Geology, 39(2), 169-191

Schwartz, T.M. and Graham, S.A., 2015. Stratigraphic architecture of a tide-influenced shelfedge delta, upper Cretaceous Dorotea Formation, Magallanes-Austral basin, Patagonia. Sedimentology 62, 1039–1077. https://doi.org/10.1111/sed.12176.

Schwartz, T.M., Fosdick, J.C. and Graham, S.A., 2016, Using detrital zircon U-Pb ages to calculate Late Cretaceous sedimentation rates in the Magallanes Austral basin, Patagonia: Basin Research., 29, 725-746.

SEGEMAR, 2003. Mapa Geológico de Santa Cruz 1:750,000. Servicio Geológico Minero de la Rep, Argentina, Buenos Aires, Argentina

SERNAGEOMIN, 2003. Mapa Geológico de Chile: versión digital, escala 1:1,000,000. Servicio Nacional de Geología y Minería, Santiago, Chile

Shultz, M.R., Fildani, A., Cope, T.D., and Graham, S.A., 2005. Deposition and stratigraphic architecture of an outcropping ancient slope system: Tres Pasos Formation. Magallanes Basin, southern Chile: Geological Society of London Special Publications, 244, 27-50.

Sickmann, Z.T., Schwartz, T.M. and Graham S.A., 2018. Refining stratigraphy and tectonic history using detrital zircon maximum depositional age: an example from the Cerro Fortaleza Formation, Austral Basin, southern Patagonia. Basin Research. 30, 708–729. https://doi.org/10.1111/bre.12272.

Sohn, Y.K., Choe, M.Y., and Jo, H.R., 2002. Transition from debris flow to hyperconcentrated flow in a submarine channel (the Cretaceous Cerro Toro Formation, southern Chile). Terra Nova, 14(5), 405-415.

Suárez, R., González, P.D., and Ghiglione, M.C., 2019. A review on the tectonic evolution of the Paleozoic-Triassic basins from Patagonia: Record of protracted westward migration of the pre-Jurassic subduction zone. Journal of South American Earth Sciences, 102256.

Sussenberger, A., Schmidt, S.T., Wemmer, K., Baumgartner, L.P. and Grobety, B., 2018. Timing and thermal evolution of fold-and-thrust belt formation in the Ultima Esperanza District, 51°S Chile: constraints from K-Ar dating and illite characterization. GSA Bulletin. 130, 975–998. https://doi.org/10.1130/B31766.1.

Sweeney, J.J., and Burnham, A.K., 1990. Evaluation of a simple model of vitrinite reflectance based on chemical kinetics. AAPG bulletin, 74(10), 1559-1570.

Thomas, C.R., 1949. Geology and Petrolum Exploration in Magallanes Province, Chile. AAPG Bulletin, 33(9): 1553-1578.

Thomson, S.N., Brandon, M.T., Tomkin, J.H., Reiners, P.W., Vásquez, C., and Wilson, N.J., 2010. Glaciation as a destructive and constructive control on mountain building. Nature, 467(7313), 313-317.

Wilson, T.J., 1983. Stratigraphic and structural evolution of the Ultima Esperanza foreland fold-thrust belt, Patagonian Andes, southern Chile (Doctoral dissertation, Columbia University).

Wilson, T.J., 1991. Transition from back-arc to foreland basin development in the southernmost Andes: stratigraphic record from the Ultima Esperanza District, Chile. GSA Bulletin. 103, 98–111. https://doi.org/10.1130/0016-7606(1991)

Winn Jr., R.D. and Dott Jr., R.H., 1979. Deep-water fan-channel conglomerates of Late Cretaceous age, southern Chile. Sedimentology 26, 203–228. https://doi.org/10.1111/j.1365-3091.1979.tb00351.x.